ARTICLES

Dynamics of H Atom Formation in the Photodissociation of Chloromethanes at 193.3 nm

Richard A. Brownsword, Matthias Hillenkamp, Thomas Laurent, Rajesh K. Vatsa,† Hans-Robert Volpp,* and Jürgen Wolfrum

Physikalisch-Chemisches Institut der Universität Heidelberg, Im Neuenheimer Feld 253, D-69120 Heidelberg, Germany

Received: November 15, 1996; In Final Form: March 28, 1997[⊗]

Using the laser photolysis/vacuum−ultraviolet laser-induced fluorescence (LP/VUV−LIF) "pump-and-probe" technique the dynamics of H atom formation after photoexcitation of chloromethanes at 193.3 nm were studied in the gas phase at room temperature under collision-free conditions. For all chloromethanes, H atoms were detected by ($2p^2P \leftarrow 1s^2S$)-LIF using tunable narrow-band Lyman-α laser radiation ($\lambda_{L\alpha} \approx 121.6$ nm) generated by resonant third-order sum−difference frequency conversion of pulsed-dye-laser radiation. However, only in the cases of CH_3Cl and CH_2Cl_2 were the H atoms found to originate from a primary photodissociation step. Absolute quantum yields for the formation of primary H atoms were measured by means of a calibration method to be $\phi_H(CH_3Cl) = (1.2 \pm 0.6) \times 10^{-2}$ and $\phi_H(CH_2Cl_2) = (0.2 \pm 0.1) \times 10^{-2}$. From H atom Doppler profiles measured under single-collision conditions, the average translational energy released to the H + CH_2Cl and H + $CHCl_2$ products in the center-of-mass system was determined to be: $E_T(H-CH_2Cl) = (86.6 \pm 14.2)$ kJ/mol and $E_T(H-CHCl_2) = (84.3 \pm 8.9)$ kJ/mol. On the basis of available thermochemical data, the corresponding fraction of the available energy released as product translational energy was determined to be $f_T(H-CH_2Cl) = (0.44 \pm 0.07)$ and $f_T(H-CHCl_2) = (0.41 \pm 0.04)$. In the $CHCl_3$ photodissociation, primary H atom formation was not observed. The H atoms detectable after laser irradiation of $CHCl_3$ at 193.3 nm were found to originate from secondary photodissociation of the $CHCl_2$ radical.

I. Introduction

The photochemistry of halogenated methanes has been of great interest ever since it was recognized that chloromethanes in the stratosphere may release Cl atoms upon absorption of solar radiation and the Cl atom so produced may catalytically decompose ozone.[1,2]

For the chloromethanes optical vacuum−ultraviolet (VUV) and ultraviolet (UV) absorption spectra,[3−6] photoelectron spectra,[7,8] and fluorescence yields after photodissociative VUV−excitation[9] have been measured. The UV−multiphoton dissociation of chlorinated methanes has been studied[10], and the VUV photolysis of $CHCl_3$[11] and UV−multiphoton ionization of CH_3Cl and CH_2Cl_2[12] has been investigated in matrices.

The VUV and UV gas phase photodissociation dynamics of the chlorinated methanes have been studied by several groups using different experimental techniques. Photofragment translational spectroscopy was used to investigate the dissociation dynamics of CH_3Cl[13,14] and $CHCl_3$[15] at a photolysis wavelength of 193.3 nm. In neither study was HCl molecular elimination or, in case of $CHCl_3$, molecular elimination of Cl_2 observed, and it was suggested that single C−Cl bond fission is the primary photolytic process for both compounds. At photolysis wavelengths of 193.3 and 157.6 nm, ground state Cl($^2P_{3/2}$) atoms and electronically excited Cl*($^2P_{1/2}$) atoms could be detected and [Cl*($^2P_{1/2}$)]/[Cl($^2P_{3/2}$)] fine structure branching ratios were measured for the chloromethanes using (2 + 1) resonance-enhanced multiphoton ionization (REMPI)[16−18] and the laser-induced fluorescence (LIF) technique[19] for Cl* and Cl atom detection. The measured Cl*/Cl branching ratio values are summarized in ref 20. For CH_3Cl and CH_2Cl_2 it was found that the Cl*/Cl branching ratio increases in going from a photolysis wavelength of 193.3 nm to a photolysis wavelength of 157.6 nm, while for $CHCl_3$, within the experimental uncertainty, no dependence on the photolysis wavelength was observed.

The formation of H atoms was observed in the 157.6 nm photolysis of chlorinated methanes[21] and relative [H]/[Cl* + Cl] yields were measured which were found to decrease with the number of H atoms present in the molecule.[22] In these studies, bimodal H atom Doppler line shapes were observed which could be described by a superposition of a Gaussian and a non-Gaussian profile.[22] The presence of two distinct H atom velocity distributions was explained by the possibility for the CH_nCl_{4-n} molecules to undergo both a direct and indirect photolytic C−H bond scission at 157.6 nm.

Recently, the dissociation dynamics of the H atom formation channel were investigated after photoexcitation of chloromethanes at the Lyman-α wavelength (∼121.6 nm) and absolute H atom quantum yields of $\phi_H(CH_3Cl) = (0.53 \pm 0.05)$, $\phi_H(CH_2Cl_2) = (0.28 \pm 0.03)$, and $\phi_H(CHCl_3) = (0.23 \pm 0.03)$ were reported.[23] In the case of CH_3Cl the measured H atom Doppler profiles showed a pronounced bimodal structure, while for CH_2Cl_2 and $CHCl_3$ the H atom Doppler line shapes could each be well-described by a single Gaussian function, which corresponds to Maxwell−Boltzmann-like translational energy distributions. At both photolysis wavelengths (157.6 nm and 121.6 nm) at which in the chloromethane dissociation H atom

† On sabbatical leave from Chemistry Division, Bhabha Atomic Research Centre, Bombay, India.

* To whom correspondence should be addressed.

[⊗] Abstract published in *Advance ACS Abstracts,* June 15, 1997.

S1089-5639(96)03811-X CCC: $14.00

formation was observed, valence, as well as Rydberg, transitions can be excited. For the chloromethanes, excitation in the first absorption band (denoted as A band in ref 5), located in the wavelength region 220−170 nm, can be described by a $3p\pi \rightarrow \sigma^*$(C−Cl) valence shell transition, where $3p\pi$ is a lone pair orbital of the Cl and σ^* is an antibonding C−Cl σ-MO. Absorption in the B and D bands which occurs at shorter wavelengths (<170 nm) was assigned to $3p\pi \rightarrow$ 4s,p Rydberg transitions.[5] In ref 14, on the basis of the results obtained in CH_3X (X = Cl, Br, and I) photodissociation studies at different photolysis wavelengths, it was suggested that for methyl halides C−H bond fission is correlated with excitation to a Rydberg-state which has a lifetime long enough to allow electronic energy transfer from the initially excited C−X bond to one of the three C−H bonds.

The aim of the present study was a systematic investigation of the chloromethanes' H atom formation dynamics after selective valence shell excitation. A photolysis wavelength of 193.3 nm was therefore chosen which allows excitation in the long-wavelength tail of the respective A bands.

II. Experimental Section

The photodissociation studies were carried out in a flow reactor at milliTorr level pressures under collision-free conditions using an apparatus similar to that used in previous VUV/UV−photodissociation[23,24] and reaction dynamics experiments.[25]

Room temperature CH_3Cl (>99.8%, Messer Griesheim), CH_2Cl_2 (>99.5%, Fluka Chemie, amylene stabilized) and $CHCl_3$ (99.8%, Riedel-de Häen, CHROMASOLV, amylene stabilized) was pumped through the reactor. The CH_3Cl flow was started several minutes before the experiments in order to ensure the removal of the small amounts of impurities, which were stated by the manufacturer to be mainly HCl and CH_4, and higher hydrocarbons, all of them having a considerable higher vapor pressure than $CHCl_3$. The liquids CH_2Cl_2 and $CHCl_3$ were degassed prior to the measurements by freeze−pump−thaw cycling at liquid N_2 temperature. In test runs with ethanol-stabilized CH_3Cl (0.5−1% ethanol) it was found that in this case the H atom signal observed was dominated by H atoms from ethanol photolysis. This was verified by a comparison of the observed H atom Doppler profiles with those obtained by photolyzing a sample of pure ethanol (>99.8%, Riedel-de Häen). Using amylene-stabilized CH_2Cl_2 and $CHCl_3$ samples no H atom signal due to ethanol photolysis could be observed.

The CH_3Cl flow was controlled by a Tylan flowmeter. CH_2Cl_2 and $CHCl_3$ flows were controlled using a needle valve. For the calibration measurement, HCl (99.999%) was passed through the reactor. The HCl flow was also controlled by a needle valve. Typical chloromethane pressures during the photodissociation experiments were 35−70 mTorr, measured by an MKS Baratron. The HCl pressure used in the calibration runs was typically 15−20 mTorr. The gases flowed through the reactor at a rate high enough to ensure renewal of the gas between successive laser shots. All measurements were carried out at a laser repetition rate of 6 Hz.

An ArF excimer laser (λ_{pump} = 193.3 nm) was used to photodissociate the chloromethanes as well as HCl. A circular aperture was used to skim off a homogeneous part of the rectangular excimer laser profile in order to provide the photolysis beam. In some of the experiments a cylindrical lens (1 m focal length) was used to partially focus the photolysis beam. Intensities were typically between 2−10 mJ/cm^2 (fluences were between 0.2×10^{16} cm^{-2} and 1×10^{16} cm^{-2}). The pump laser beam was determined to be essentially unpolarized, and it is therefore expected that any possible anisotropy of the photodissociation process would be largely averaged out.

Tunable Lyman-α-laser light (λ_{probe} = 121.567 nm) for H atom detection via ($2p^2P \leftarrow 1s^2S$) laser-induced fluorescence was generated by resonant third-order sum−difference frequency conversion ($\omega_{VUV} = 2\omega_R - \omega_T$) in a Kr−Ar mixture.[26] The fixed frequency ω_R (λ_R = 212.55 nm) was resonant with the Kr two-photon transition 4p−5p (1/2, 0), while the frequency ω_T was tuned from 844 to 845.5 nm to cover the H atom Lyman-α transition. The "primary" laser radiation for the nonlinear mixing process was obtained from two tunable dye lasers, simultaneously pumped by a XeCl excimer laser, one of which, ω_R, was frequency doubled with a BBO II crystal. The generated Lyman-α light was carefully separated from the fundamental laser light by a lens monochromator followed by a light baffle system. A bandwidth of $\Delta\nu \approx 0.4$ cm^{-1} was determined for the Lyman-α laser radiation in separate experiments by measuring Doppler profiles of H atoms (generated by a microwave discharge) under thermalized conditions ($T \approx$ 300 K).

The photolysis laser beam was aligned so as to overlap the probe beam at right angles in the viewing region of the LIF detector. The delay time between the pump and probe pulse was typically (100 ± 5) ns. The LIF signal was measured through a band-pass filter by a solar blind photomultiplier positioned at right angles to both pump and probe laser. In order to obtain a satisfactory S/N ratio, each point of the H atom Doppler profiles was averaged over 30 laser shots. During the experiments, the change of the intensity of the probe laser beam was monitored with an additional solar blind photomultiplier of the same kind. The H atom LIF signal, Lyman-α probe beam, and the photolysis laser intensities were recorded with a three-channel boxcar system and transferred to a microcomputer, via an analogue-to-digital converter, where the LIF signal was normalized to both photolysis and probe laser intensities.

A contribution to the LIF signal from H atoms produced directly by the Lyman-α photolysis of the chloromethanes was observed.[23] Although the probe laser fluence was considerably lower (typically 1×10^{12} cm^{-2}) than in the experiments carried out in ref 23, an electronically controlled mechanical shutter was inserted into the photolysis beam path in order to discriminate between the residual "Lyman-α-background" H atom signal and that from H atoms produced by the 193.3 nm photolysis laser. At each point of the H atom Doppler profile, signal was recorded first with the shutter open, and then with the shutter closed, the difference between the two signals was obtained using a point-by-point subtraction procedure. This allowed to obtain a Doppler profile free from the H atom background produced via the probe laser photolysis of CH_3Cl, CH_2Cl_2, and $CHCl_3$.

III. Results and Discussion

A. CH_3Cl, CH_2Cl_2: Absolute Quantum Yield for Primary H Atom Formation. At the UV wavelength of 193 nm, CH_3Cl and CH_2Cl_2 have rather low optical absorption cross sections[3c,10] of 6.96×10^{-20} and 3.7×10^{-19} cm^2, respectively. In order to verify that the H atoms observed in the CH_3Cl and CH_2Cl_2 photodissociation originate from primary dissociation processes, the dependence of the H atom signal on the intensity of the photolysis and probe laser was investigated. For both molecules, within the experimental uncertainty, a linear dependence of the measured H atom signal on the photolysis ("pump") and probe laser intensities was observed (see e.g., Figure 1a,b) consistent with the following primary dissociation steps

$$CH_3Cl + \hbar\omega(193.3\ \text{nm}) \rightarrow CH_2Cl + H \qquad (1)$$

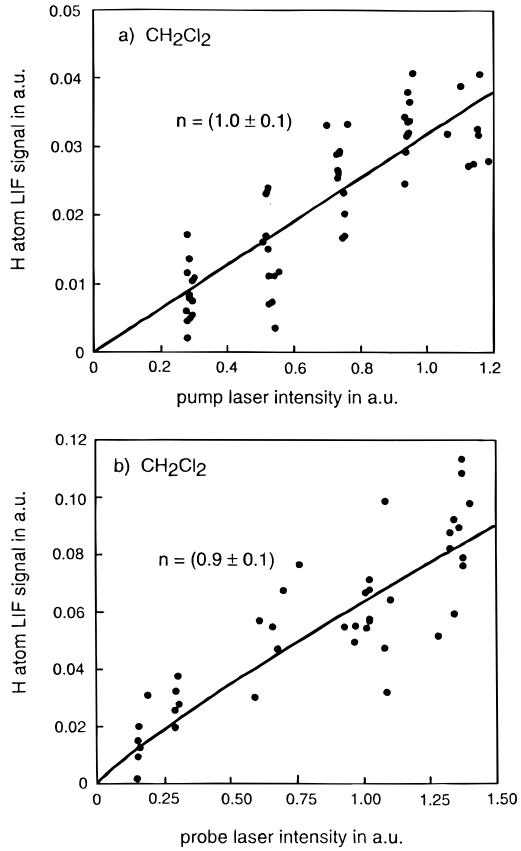

Figure 1. Dependence of the observed H atom LIF signal: (a) on the photolysis "pump" laser (193.3 nm) and (b) Lyman-α "probe" laser intensity for CH_2Cl_2. The solid lines represent the results of a fit assuming a I^n dependence of the H atom LIF signal on the pump and probe laser intensity, respectively. The obtained numerical values for n are given in the figure.

$$CH_2Cl_2 + \hbar\omega(193.3\text{ nm}) \rightarrow CHCl_2 + H \qquad (2)$$

followed by a single-photon H atom VUV-LIF detection step.

An alternative route of H atom formation via a two-photon (193 nm) two-step photodissociation mechanisms where both photons are absorped in the same pump laser pulse

$$CH_3Cl + \hbar\omega(193.3\text{ nm}) \rightarrow CH_3 + Cl \qquad (3a)$$

$$CH_3 + \hbar\omega(193.3\text{ nm}) \rightarrow CH_2 + H \qquad (3b)$$

$$CH_2Cl_2 + \hbar\omega(193.3\text{ nm}) \rightarrow CH_2Cl + Cl \qquad (4a)$$

$$CH_2Cl + \hbar\omega(193.3\text{ nm}) \rightarrow CHCl + H \qquad (4b)$$

could also lead, if the second steps 3b and 4b would be saturated, to a linear dependence of the measured H atom signal on the pump laser intensity. However, because of the low pump laser fluences $f = (0.2-1) \times 10^{16}$ cm^{-2} employed in the experiments, saturation of 3b and (4b) is rather unlikely, although the CH_3 and CH_2Cl radicals are expected to have higher optical absorption cross sections than the parent molecules. UV absorption cross sections for the CH_3 and CH_2Cl radicals were measured by different groups.[27−29] Values of $\sigma_{CH_3}(200\text{ nm}) = 1.6 \times 10^{-19}$ cm^{-2} and $\sigma_{CH_2Cl}(198.5\text{ nm}) = 13.1 \times 10^{-18}$ cm^{-2} were reported in refs 28 and 29. In both cases, even for the maximum pump laser fluence the product $f_{max}\sigma_{CH_3} = 0.0016$ and $f_{max}\sigma_{CH_2Cl} = 0.13$ is well below unity, and therefore saturation of the steps 3a and 4b is not possible. As a consequence, if reaction sequences 3 and 4 would contribute significantly to H atom formation, a deviation from a linear pump laser power dependence is expected. Although a pronounced deviation was not observed—after calibration of the H atom signal—the H atom quantum yield of the secondary photodissociation step which would be consistent with the uncertainty of the measured linear pump laser power dependence (see, e.g., Figure 1a) and the corresponding contribution of secondary photolysis to the overall H atom yield can be estimated.

On the other hand, should secondary photolysis of CH_3 and CH_2Cl radicals by the probe laser contribute significantly to H atom formation, the H atom signal would exhibit a square dependence on the probe laser intensity, unless the radical probe photolysis step is saturated. The lattter would require, because of the very low probe laser fluence of about 1×10^{12} cm^{-2} used in the present experiments, VUV absorption cross sections $\sigma_{CH_3}(121.6\text{ nm})$ and $\sigma_{CH_2Cl}(121.6\text{ nm})$ of $\sim 10^{-12}$ cm^2, which seem to be unreasonably high.

In addition, different test runs were carried out in which the delay time between the pump and probe laser pulse was varied between 80 and 150 ns. No significant change in the H atom signal was observed, consistent with production of H atoms solely by photolysis rather then chemical side reactions of photolysis products.

Absolute H atom quantum yields ϕ_H were obtained by calibrating the H atom signal $S_H(RX)$ measured in the chloromethane photodissociation against the H atom signal $S_H(HCl)$ from well-defined H atom number densities generated by photolyzing HCl. The values for the absolute H atom quantum yields were calculated using the following equation:

$$\phi_H = \gamma \{S_H(RX)\, \sigma_{HCl} p_{HCl}\}/\{S_H(HCl)\, \sigma_{RX} p_{RX}\} \qquad (5)$$

where S is the integrated area under the measured H atom Doppler profiles. p_{HCl} and p_{RX} are the pressure of HCl and the chloromethanes, respectively. σ_{HCl} and σ_{RX} are the optical absorption cross sections of HCl and the chloromethanes at 193.3 nm. The optical absorption cross section of HCl at 193.3 nm has been measured[30] to be $(8.1 \pm 0.4) \times 10^{-20}$ cm^2. For CH_3Cl and CH_2Cl_2, values for the optical absorption cross section of 6.96×10^{-20} and 3.7×10^{-19} cm^2 were reported in refs 3c and 10, respectively, for the 193.3 nm wavelength. In eq 5, the factor γ is a correction which accounts for the different degrees of absorption of the Lyman-α probe laser radiation by CH_3Cl/CH_2Cl_2 and HCl. Optical absorption cross sections for CH_3Cl and CH_2Cl_2 at the Lyman-α wavelength were reported to be $(8.8 \pm 0.2) \times 10^{-17}$ and $(4.0 \pm 0.1) \times 10^{-17}$ cm^2, respectively.[23] In the case of HCl, the absorption of the Lyman-α probe laser radiation was negligible under our experimental conditions.

Figure 2 shows typical H atom Doppler profiles obtained in the 193.3 nm photodissociation of CH_3Cl, CH_2Cl_2, and HCl. In independent calibration runs, integrated areas under the fluorescence curves were determined under identical experimental conditions which gave, using eq 5, the following average values for the H atom quantum yields: $\phi_H(CH_3Cl) = (1.2 \pm 0.6) \times 10^{-2}$ and $\phi_H(CH_2Cl_2) = (0.2 \pm 0.1) \times 10^{-2}$.

As mentioned above, from the experimental uncertainty (2σ of the least-squares-fit result) in the H atom versus pump laser intensity plots, one can estimate using the available literature values for the CH_3 and CH_2Cl absorption cross sections the corresponding maximum "secondary" H atom quantum yield and hence the maximum contribution of secondary photolysis. For CH_3Cl, because of the very small absorption cross sections of CH_3, only a small number of the CH_3 radicals are actually photolyzed at the pump fluences of the experiment and therefore

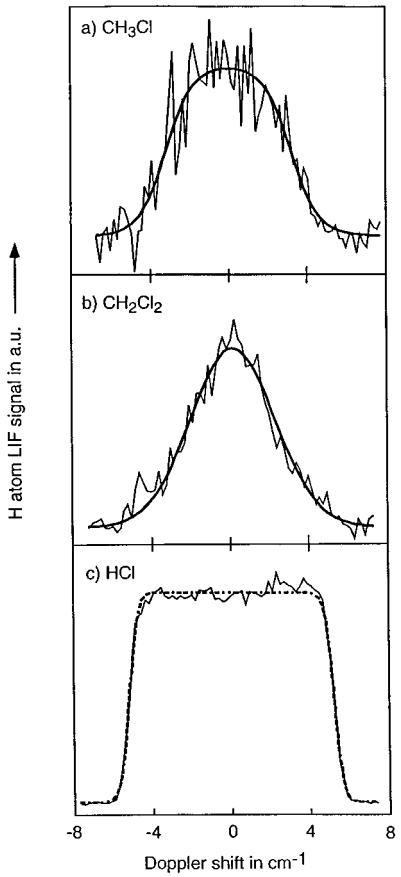

Figure 2. H atom Doppler profiles obtained in the 193.3 nm photolysis: (a) CH_3Cl (50.3 mTorr). The solid line represents the result of a fit of a symmetric double sigmoidal function. (b) CH_2Cl_2 (57.5 mTorr). Here the solid line represents the result of a fit using a Gaussian function. (c) HCl (17.3 mTorr). The centers of the LIF spectra correspond to the Lyman-α transition of the H atom (82 259 cm^{-1}).

even for a quantum yield of unity the contribution of the so produced secondary H atoms (which exhibits a square dependence on the pump laser fluence) cannot lead to pronounced deviation from a linear pump laser power dependence. The maximum contribution of secondary H atoms to the measured signal is estimated to be ∼10%. However, in case of CH_2Cl_2, because of the much higher absorption cross section of the CH_2Cl radical, the observed linear pump laser power dependence (1.0 ± 0.2) clearly restricts the possible H atom quantum yield in the 193.3 nm photolysis of the CH_2Cl radical to ∼1%, which is consistent with HCl elimination being the main product channel in the CH_2Cl secondary photolysis. In case of CH_2Cl_2 photolysis, the maximum possible contribution of secondary photodissociation to the observed H atom signal which is consistent with the experimental pump laser power dependence of (1.0 ± 0.2) is estimated to be ∼30% at the highest fluence used in the experiment.

In Table 1, the experimental results are summarized and compared to primary H atom yields obtained at shorter photolysis wavelengths.[21,23] A similar trend was observed in early alkyl iodide flash photolysis experiments by Levy and Simons[31] where they found that at long wavelengths (>170 nm) the quantum yield of C−H bond scission is quite small (<10^{-2}), while at shorter wavelengths C−H rather than C−I bond scission is going to become the dominating photodissociation process.

B. CH_3Cl, CH_2Cl_2: Average H Atom Translational Energy. The H atom Doppler profiles were evaluated in order to determine the fraction of the average available energy released as relative H−CH_2Cl and H−$CHCl_2$ translational energy after photoexcitation of CH_3Cl and CH_2Cl_2 at 193.3 nm. The average kinetic energy of the H atoms was calculated directly from the measured profiles by fitting an analytical function to the observed Doppler lineshapes (see Figure 2) in order to calculate the second moment of the laboratory velocity distribution. The following values for the translational energy and, based on the thermochemical data compiled in ref 32 (see Table 2), the fraction of the available energy released into the relative translational degree of freedom were determined to be E_T(H−CH_2Cl) = (86.6 ± 14.2) kJ/mol, E_T(H−$CHCl_2$) = (84.3 ± 8.9) kJ/mol and f_T(H−CH_2Cl) = (0.44 ± 0.07), f_T(H−$CHCl_2$) = (0.41 ± 0.04), respectively. A comparison of the latter values with the results of a statistical "prior" calculation,[33,34] which yields f_T^{prior} (H−CH_2Cl) = f_T^{prior} (H−$CHCl_2$) ≈ 0.17, indicates that in the photodissociation process the available energy is partitioned in a nonstatistical fashion.

TABLE 1: Comparison of Primary H Atom Quantum Yields ϕ_H Obtained in the Photolysis of Chloromethanes

molecule	λ_{photo}/nm	ϕ_H
CH_3Cl	193.3	$(1.2 \pm 0.6) \times 10^{-2}$
	157.6	0.29[a]
	121.6[b]	(0.53 ± 0.05)
CH_2Cl_2	193.3	$(0.2 \pm 0.1) \times 10^{-2}$
	157.6	0.23[a]
	121.6[b]	(0.28 ± 0.03)
$CHCl_3$	193.3	≈0
	157.6	0.13[a]
	121.6[b]	(0.23 ± 0.03)

[a] The ϕ_H values at 157.6 nm were calculated from the relative H versus Cl atom yields given in ref 21 assuming that $\phi_H + \phi_{Cl+Cl^*} = 1$. [b] Results for the photolysis wavelength at 121.6 nm are from ref 23.

TABLE 2: Standard Enthalpies of Formation ΔH°_f (298 K) and Reaction Enthalpies ΔH_R of Different Product Channels in kJ/mol[a]

species	ΔH°_f(298 K)	reaction	ΔH_R(298 K)	E_{avl}
CH_3Cl	−82	$CH_3Cl \rightarrow CH_2Cl + H$	421	197
CH_2Cl_2	−95.4	$CH_2Cl_2 \rightarrow CHCl_2 + H$	411.7	207.2
$CHCl_3$	−103.3	$CHCl_3 \rightarrow CCl_3 + H$	392.4	226.5
CH_2Cl	121.8	$CHCl_3 \rightarrow CHCl_2 + Cl$	322.9	296.0
$CHCl_2$	98.3	$CHCl_3 \rightarrow CHCl_2 + Cl^*$	332.5	286.3
CCl_3	71.1	$CHCl_2 \rightarrow CCl_2 + H$	358	
CCl_2	239			
Cl/Cl*	121.30/130.94[b]			
H	217.997			

[a] From ref 32. For primary dissaciation channels the available energy to the products is given by $E_{avl} = \omega_{193.3nm}$ (618.9 kJ/mol)−ΔH_R (298 K). [b] ΔH°_f (298 K) of Cl* has been calculated using ΔE = 0.1 eV (kJ/mol) for the Cl ($^2P_{1/2-3/2}$) spin−orbit splitting.

C. $CHCl_3$: Secondary H Atom Formation in the 193.3 nm Photolysis. In the case of $CHCl_3$, the observed H atom signal showed a quadratic dependence on the pump laser intensity (Figure 3a). In these measurements the pump laser beam was unfocused with the highest intensity being about 2 mJ/cm^2. In measurements with a slightly focused pump laser beam with intensities up to 10 mJ/cm^2 the same quadratic pump laser power dependence was observed.

For the probe laser, an almost linear H atom signal versus intensity dependence was found (Figure 3b). The observed pump and probe laser intensity dependencies would be consistent with the following sequential two-photon dissociation mechanism

$$CHCl_3 + \hbar\omega(193.3\ nm) \rightarrow CHCl_2 + Cl/Cl^* \quad (6a)$$

$$CHCl_2^{\ddagger} + \hbar\omega(193.3\ nm) \rightarrow H + CCl_2 \quad (6b)$$

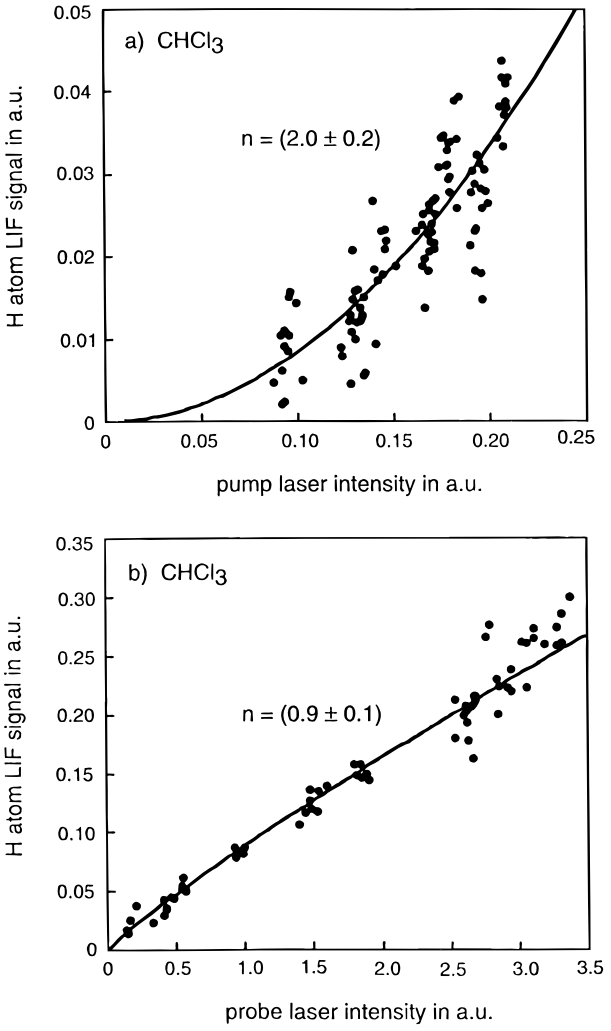

Figure 3. Dependence of the observed H atom LIF signal: (a) on the photolysis "pump" laser (193.3 nm) and (b) Lyman-α "probe" laser intensity for $CHCl_3$. The solid lines represent the results of a fit assuming a I^n dependence of the H atom LIF signal on the pump and probe laser intensity, respectively. The obtained numerical values for n are given in the figure.

where the H atoms are produced by secondary photolysis of internally excited $CHCl_2$ radicals within the same pump laser pulse followed by a single-photon H atom LIF detection step.

A direct two-photon dissociation mechanism

$$CHCl_3 + 2 \times \hbar\omega(193.3\ \text{nm}) \rightarrow H + ... \qquad (7)$$

which could give rise to the same pump laser intensity dependence seems to be rather improbable at the low pump laser fluences of the present study. The product of the pump laser fluence ($\sim 2 \times 10^{15}$ cm^{-2}) and the optical absorption cross section of $CHCl_3$ at 193.3 nm (8.3×10^{-19} cm^2)[10] is well below unity.

In Figure 4, a typical H atom Doppler profile as observed in the $CHCl_3$ photolysis experiments is depicted where the solid line represents the result of a fit using a Gaussian function. The corresponding fragment translational energy was determined to be (82.6 ± 9.0) kJ/mol.

Chlorine atom formation after excitation of $CHCl_3$ at 193.3 nm has been investigated in great detail.[15,18,35] For the primary dissociation step 6a the Cl*/Cl branching ratio has been measured to be 0.25[20] and the fragment kinetic energy has been reported to be 130 kJ/mol.[15] These results can be used to determine the average internal energy of the $CHCl_2$ fragments

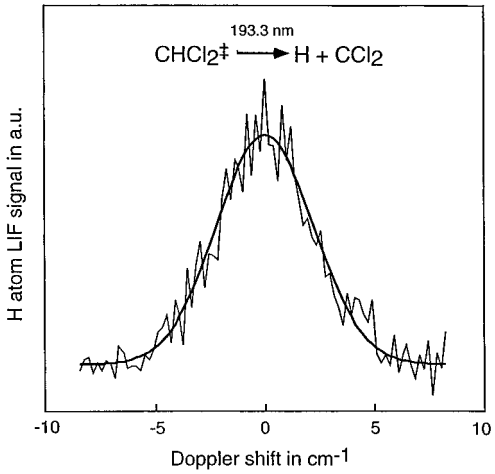

Figure 4. Doppler line shape of H atoms formed by the secondary photolysis of $CHCl_2$ fragments produced in the 193.3 nm photolysis of $CHCl_3$. As in Figure 2, the center of the Doppler profile corresponds to the Lyman-α transition of the H atom (82 259 cm^{-1}).

produced via (4a) to be $E_{int}(CHCl_2) = 163$ kJ/mol. Using this value the fraction of the available energy which shows up in the H−CCl_2 translational degree of freedom can be calculated to be f_T(H-CCl_2) = (0.19 ± 0.03) for the dissociation step 6b. The error of the f_T value was calculated from the uncertainty of the fragment translational energies of eqs 6a and 6b using simple error propagation. The experimental uncertainty in the measurement of the fragment translational energy of eq 6a was assumed to be similar to the one of eq 6b of the present study (∼10%). A comparison with the corresponding statistical prior value of f_T^{prior} (H−CCl_2) = 0.25, calculated taking into account energy conservation only,[32,33] might suggest that the intermediate formed by photoexcitation of the $CHCl_2$ radicals decomposes via eq 6b by a statistical unimolecular decay with a lifetime long enough to allow for almost complete internal energy redistribution. In a recent study on the unimolecular decomposition of $CHCl_2$ radicals, a Cl formation and HCl elimination pathway could also be observed.[36]

IV. Conclusions

The H atom formation channel after photoexcitation of chloromethanes at a wavelength of 193.3 nm was investigated. The rather low H atom yields observed in the present studies show that dissociation of CH_3Cl and CH_2Cl_2 after photoabsorption at 193.3 nm, where $3p\pi \rightarrow \sigma^*$(C−Cl) valence shell transitions are excited, does not result in efficient primary C−H bond cleavage. Comparison with earlier measurement confirms that primary photolytic H atom production becomes increasingly important in going to shorter photodissociation wavelengths. The observed nonstatistical energy partitioning could be explained by a H atom formation mechanism taking place on a time scale which does not allow for complete internal energy redistribution of the photolytically prepared intermediate.

In case of $CHCl_3$, primary H atom formation could not be observed after photoexcitation at 193.3 nm. H atoms detectable in the experiments were found to originate from secondary photolysis of $CHCl_2$ radicals which are generated as primary products in the photodissociation of $CHCl_3$. The observed energy partitioning suggests that the secondary H atom formation proceeds via statistical unimolecular decay of the $CHCl_2$ radical upon absorption of a 193.3 nm photon.

Acknowledgment. R.K.V. acknowledges a fellowship and its extension provided by the KFA Jülich and the DLR-Bonn

under the Indo-German bilateral agreement (Project CHEM-19). The authors gratefully acknowledge financial support of the European Union under Contract ISC*-CT940096 of the International Scientific Cooperation programme between the University of Heidelberg and the Ben-Gurion-University of the Negev (Beer-Sheva, Israel) as well as support of the Deutsche Forschungsgemeinschaft. Professor M. Kawasaki is thanked for prompt and helpful communications.

References and Notes

(1) Crutzen, P. J. In *Physics and Chemistry of Upper Atmospheres*; McCormac, B. M., Ed.; Reidel: Dordrecht, 1973.

(2) Molina, M. J.; Rowland, F. S. *Nature* **1974**, *249*, 810. Rowland, F. S.; Molina, M. J. *Rev. Geophys. Space Phys.* **1975**, *13*, 1.

(3) (a) Russel, B. R.; Edwards, L. O.; Raymonda, J. W. *J. Am. Chem. Soc.* **1973**, *95*, 2129. (b) Robbins, D. E. *Geophys. Res. Lett.* **1976**, *3*, 213. (c) Hubrich, C.; Zetzsch, C.; Stuhl, F. *Ber. Bunsen-Ges. Phys. Chem.* **1977**, *81*, 437.

(4) Tsubomura, H.; Kimura, K.; Kaya, K.; Tanaka, J.; Nagakura, S. *Bull. Chem. Soc. Jpn.* **1964**, *37*, 417.

(5) Robin, M. B. *Higher Excited States of Polyatomic Molecules*; Academic Press: New York, 1974, Vol. I.

(6) Okabe, H. *Photochemistry of Small Molecules*; John Wiley & Sons: New York, 1978.

(7) Potts, A. W.; Lempka, H. J.; Streets, D. G.; Price, W. C. *Philos. Trans. R. Soc. London* **1970**, *268A*, 59.

(8) Zhang, W.; Cooper, G.; Ibuki, T.; Brion, C. E. *Chem. Phys.* **1989**, *137*, 391. Olney, T. N.; Chan, W. F.; Cooper, G.; Brion, C. E.; Tan, K. H. *J. Electron Spectrosc. Relat. Phenom.* **1993**, *66*, 83. Pradeep, T.; Shirley, D. A. *Ibid.* **1993**, *66*, 125.

(9) Lee, L. C.; Suto, M. *Chem. Phys.* **1987**, *114*, 423.

(10) Haak, H. K.; Stuhl, F. *Chem. Phys. Lett.* **1979**, *68*, 399.

(11) Jacox, M. E.; Milligan, D. E. *J. Chem. Phys.* **1971**, *54*, 3935.

(12) Machara, N. P.; Ault, B. S. *J. Phys. Chem.* **1989**, *93*, 1908.

(13) Kawasaki, M.; Kasatani, K.; Sato, H.; Shinohara, H.; Nishi, N. *Chem. Phys.* **1984**, *88*, 135.

(14) Continetti, R. E.; Balko; B. A.; Lee, Y. T. *J. Chem. Phys.* **1988**, *89*, 3383.

(15) Yang, X.; Felder, P.; Huber, J. R. *Chem. Phys.* **1994**, *189*, 127.

(16) Matsumi, Y.; Das, P. K.; Kawasaki, M. *J. Chem. Phys.* **1990**, *92*, 1696.

(17) Matsumi, Y.; Tonokura, K.; Kawasaki, M. *J. Chem. Phys.* **1990**, *93*, 7981.

(18) Matsumi, Y.; Tonokura, K.; Kawasaki, M.; Inoue, G.; Satyapal, S.; Bersohn, R. *J. Chem. Phys.* **1991**, *94*, 2669.

(19) Tonokura, K.; Matsumi, Y.; Kawasaki, M.; Tasaki, S.; Bersohn, R. *J. Chem. Phys.* **1992**, *97*, 8210.

(20) Tonokura, K.; Matsumi, Y.; Kawasaki, M.; Tasaki, S.; Bersohn, R. *J. Chem. Phys.* **1992**, *97*, 5261.

(21) Tonokura, K.; Matsumi, Y.; Kawasaki, M.; Kasatani, K. *J. Chem. Phys.* **1991**, *95*, 5065.

(22) Tonokura, K.; Mo, Y.; Matsumi, Y.; Kawasaki, M. *J. Phys. Chem.* **1992**, *96*, 6688.

(23) Brownsword, R. A.; Laurent, T.; Hillenkamp, M.; Vatsa, R. K.; Volpp, H.-R.; Wolfrum, J. *J. Chem. Phys.* **1997**, *106*, 1359.

(24) Brownsword, R. A.; Laurent, T.; Vatsa, R. K.; Volpp, H.-R.; Wolfrum, J. *Chem. Phys. Lett.* **1996**, *249*, 162. *Ibid.* **1996**, *258*, 164.

(25) Volpp, H.-R.; Wolfrum, J. In *Gas Phase Chemical Reaction Systems: Experiments and Models 100 Years after Max Bodenstein*; Springer Series in Chemical Physics 61; Wolfrum, J., Volpp, H.-R., Rannacher, R., Warnatz, J., Eds.; Springer: Heidelberg, 1996.

(26) Hilber, G.; Lago, A.; Wallenstein, R. *J. Opt. Soc. Am. B.* **1987**, *4*, 1753. Marangos, J. P.; Shen, N.; Ma, H.; Hutchison, M. H. R.; Connerade, J. P. *J. Opt. Soc. Am. B.* **1990**, *1*, 1254.

(27) Callear, A. B.; Metcalfe, M. P. *Chem. Phys.* **1976**, *14*, 275.

(28) Glänzer, K.; Quack, M.; Troe, J. *16th International Symposium on Combustion*, Massachusetts Institute of Technology, Aug 15−20, 1976; The Combustion Institute: Pittsburgh, 1977; 949.

(29) Roussel, P. B.; Lightfoot, P. D.; Caralp, F.; Catoire, V.; Lesclaux, R.; Frost, W. *J. Chem. Soc., Faraday Trans.* **1991**, *87*, 2367.

(30) Mo, Y.; Tonkua, K.; Masum, Y.; Kawasaki, M.; Sato, T.; Arikawa, T.; Reilly, P. T. A.; Xie, Y.; Yag, Y.; Huag, Y.; Gordon, R. J. *J. Chem. Phys.* **1992**, *97*, 4815.

(31) Levy, M. R.; Simons, J. P. *J. Chem. Soc., Faraday Trans. 2* **1975**, *71*, 561.

(32) Atkinson, R.; Baulch, D. L.; Cox, R. A.; Hampson, R. F., Jr.; Kerr, J. A.; Troe, J. *J. Phys. Chem. Ref. Data* **1992**, *21*, 1125.

(33) Levine, R. D.; Kinsey, J. L. In *Atom-Molecule Collision Theory—A Guide for the Experimentalist*; Bernstein, R. B., Ed.; Plenum Press: New York, 1979. Levine, R. D.; Bernstein, R. B. *Molecular Reaction Dynamics and Chemical Reactivity*; University Press: Oxford, 1987.

(34) Muckermann, J. T. *J. Phys. Chem.* **1989**, *93*, 180.

(35) Nachbor, M. D.; Giese, C. F.; Gentry, W. R. *J. Phys. Chem.* **1995**, *99*, 15400.

(36) Sadílek, M.; Tureček, F. *J. Phys. Chem.* **1996**, *100*, 224.